Journal of Climate

Dynamics of the Disrupted 2015-16 Quasi-Biennial Oscillation

--Manuscript Draft--

Manuscript Number:	JCLI-D-16-0663
Full Title:	Dynamics of the Disrupted 2015-16 Quasi-Biennial Oscillation
Article Type:	Article
Abstract:	A significant disruption of the Quasi-Biennial Oscillation (QBO) occurred during the Northern Hemisphere (NH) winter of 2015-16. Since the QBO is the major wind variability source in the tropical lower stratosphere and influences the rate of ascent of air entering the stratosphere, understanding the cause of this singular disruption may provide new insights into the variability and sensitivity of the global climate system. Here we examine this disruptive event using global reanalysis winds and temperatures from 1980-2016. Results reveal record maximums in tropical horizontal momentum fluxes and wave forcing of the tropical zonal mean zonal wind over the NH 2015-16 winter. The Rossby waves responsible for these record tropical values originated in the NH and were focused strongly into the tropics at the 40 hPa level.

Dynamics of the Disrupted 2015-16 Quasi-Biennial Oscillation

Lawrence Coy*

NASA GSFC, Greenbelt, MD, USA and SSAI, Lanham, MD, USA

Paul A. Newman, Steven Pawson

NASA GSFC, Greenbelt, MD, USA

Leslie R. Lait

NASA GSFC, Greenbelt, MD, USA and Morgan State University, MD, USA

**Corresponding author address:* Lawrence Coy, NASA GSFC Code 610.1, Greenbelt, MD, MD/USA.

E-mail: lawrence.coy@nasa.gov

ABSTRACT

A significant disruption of the Quasi-Biennial Oscillation (QBO) occurred during the Northern Hemisphere (NH) winter of 2015–16. Since the QBO is the major wind variability source in the tropical lower stratosphere and influences the rate of ascent of air entering the stratosphere, understanding the cause of this singular disruption may provide new insights into the variability and sensitivity of the global climate system. Here we examine this disruptive event using global reanalysis winds and temperatures from 1980–2016. Results reveal record maximums in tropical horizontal momentum fluxes and wave forcing of the tropical zonal mean zonal wind over the NH 2015–16 winter. The Rossby waves responsible for these record tropical values originated in the NH and were focused strongly into the tropics at the 40 hPa level.

1. Introduction

The Quasi-Biennial Oscillation (QBO) consists of downward propagating easterly and westerly zonal wind regimes in the tropical lower stratosphere (100–10 hPa, $\sim$18–30 km in altitude) with a varying ($\sim$28 month) period (see Baldwin et al. 2001, and references therein). The QBO has been a persistent characteristic of the tropical lower stratosphere since observations began in 1953. However, a significant disruption of the QBO occurred during the Northern Hemisphere (NH) winter of 2015–16 (Newman et al. 2016) and several features of this singular disruption, as noted in Newman et al. (2016), imply that a different mechanism may have been responsible for the disrupting accelerations than the vertically propagating waves responsible for the QBO. Most noticeably, anomalous easterly accelerations occurred in the center of the QBO westerlies, a region of weak vertical wind shear, rather than in the strong vertical wind shear regions as has been typically observed. A possible source of this anomalous tropical easterly acceleration would be mid-latitude Rossby waves propagating upward from the troposphere into the stratosphere and then equatorward. Here we investigate the characteristics of the wave motions associate with this anomalous easterly acceleration.

The basic QBO mechanism is forced by vertically propagating equatorial waves (Lindzen and Holton 1968). Selective filtering of vertically propagating waves by the QBO wind distribution coupled with the tendency of the waves to break, deposit momentum, and thereby dissipate in regions of the QBO wind shear produce appropriately signed zonal wind accelerations that effectively lower the shear regions by approximately 1 km month^{-1}. Thus the strength of the wave forcing determines the QBO period. The waves responsible are a mix of global scale eastward propagating Kelvin waves, westward propagating equatorial Rossby-gravity waves and smaller scale eastward and westward propagating gravity waves, all originating in the troposphere (Holt et al. 2016). Even relatively small zonal accelerations can build strong equatorial winds over time as the lack of the Coriolis force at the equator enables the winds to continue in the direction of the acceleration rather than turning as at mid-latitudes.

In contrast to the typical downward propagation of the QBO, based on wave-induced accelerations in the regions of vertical wind shear, Newman et al. (2016) found easterlies developing in the region of strong westerlies. Since vertical propagating equatorial and gravity waves are not expected to break in this region, there is the possibility that Rossby waves, originating outside the tropics may be breaking as they encounter horizontal wind shears associated with the QBO. An upward-equatorward pattern is typical of Rossby wave propagation in the winter stratosphere (Hamilton 1982), however the effect of Rossby waves on the equatorial winds has been considered to be small based on idealized model experiments that showed Rossby waves interacting with the edges of the QBO westerly jet but not changing the magnitude of the jet (O'Sullivan 1997). Given the structure of the anomalous QBO evolution observed during 2015–16, the potential of Rossby waves to significantly affect the QBO needs to re-examined.

To characterize the wave forcing responsible for the disruption of the QBO we examine the Rossby wave equatorial momentum forcing during the 2015–16 NH winter using global reanalysis winds and temperatures from 1980–2016. After describing the data sets used and the analysis procedure (Section 2), we present the mean equatorial momentum fluxes and their divergences along with the evolution of the zonal mean zonal wind (Section 3), followed by a summary and discussion of the results (Section 4).

2. Data and Methods

For this study we use two output collections from the Modern-Era Retrospective analysis for Research and Applications-Version 2, MERRA-2 (Bosilovich et al. 2015): the 3 hourly instantaneous on model levels (GMAO 2015a) and monthly averages on constant pressure levels (GMAO 2015b). MERRA-2 begins in January 1980 and is ongoing. The stand-alone MERRA-2 model component generates its own QBO (Molod et al. 2015), thereby reducing reliance on observations for the assimilated QBO (Coy et al. 2016). Time altitude cross sections of the MERRA-2 QBO zonal mean zonal winds from 1980–2012 are shown in Kawatani et al. (2016).

A QBO composite from MERRA-2 was generated based on the date of the change from zonal mean easterlies to westerlies at 30 hPa. The zonal mean zonal winds from the 3 hour collection were averaged over a day and from 10°S–10°N before selecting the composite dates of the wind sign change. The composite QBO averages different times of year so that the annual and semi-annual cycles tend to averaged to zero, however, the specific years examined, 2014-16, have both annual and semi-annual cycles present. To compare without the annual and semi-annual cycles, the monthly averages over the years 1980-2014 were removed when constructing the deviation of 2014–16 from the composite (Fig. 1c). This procedure mainly removed a semi-annual signal at the upper levels shown. The standard deviation of the composite (Fig. 1d) was multiplied by a factor of $\sqrt{2}$ to estimate the amplitude of the variability.

The Eliassen-Palm flux vectors (EP flux, see Andrews et al. 1987, page 128) are proportional to Rossby wave meridional and vertical group velocities and amplitudes. The EP flux divergence accelerates the zonal mean zonal wind. For this study the EP flux was calculated using the monthly averaged MERRA-2 data collection. These contain the meridional heat and momentum fluxes ($\overline{v'T'}$ and $\overline{u'v'}$ where u', v', and T' are zonal wind component, meridional wind component, and temperature respectively, the prime denotes a deviation from the zonal mean, and the overbar denotes a zonal mean) needed for the EP flux calculation, however, the vertical flux of zonal wind fields, $\overline{u'w'}$ (where w is vertical velocity), is not included in the collection, so this term in the vertical component of the EP flux was neglected. This term is generally small for planetary scale waves that are being considered here and even for tropical waves, such as the Kelvin wave, and smaller scale gravity waves, the EP flux convergence should be small in the region of interest near 40 hPa since the vertical wind shear is small there during the 2015–16 winter, suggesting little wave breaking and dissipation of these vertically propagating waves. Plotting the EP flux vectors can be problematic as they decrease in amplitude at upper levels and in the tropics. To address this issue they are plotted only over a limited altitude (70 hPa and above) and latitude (30°S-30°N) range.

Along with the EP flux vector, we examine the heat and momentum fluxes. Since the tropical momentum and heat fluxes are generally an order of magnitude smaller than their winter middle latitude values and decrease with altitude, we have normalized these fluxes by their local standard deviations when comparing their relative values from during individual years. The monthly averaged heat and momentum fluxes (GMAO 2015b) were first zonally averaged and then the mean and standard deviations were calculated at each latitude and vertical level over the MERRA-2 time period (1980-2014, 36 or 37 monthly averaged values). After subtracting the multi-year monthly mean, the fluxes were then divided by the monthly standard deviation for each location, providing normalized values in terms of the local standard deviations.

The response of the mean meridional circulation to the disrupted QBO was examined calculating the residual mean meridional circulation and plotting the vertical component, $\overline{w}^*$, using the same data sets as in the EP flux calculation described above. To focus on the perturbation the multi-year monthly average values (Dec 1981 – Feb 2015) were subtracted from each month before averaging for the winter season (Dec 2015 – Feb 2016).

3. Results

The 2015-16 QBO was highly disrupted from its normal behavior. Figure 1 illustrates the time height structure of the MERRA-2 zonal mean zonal wind (Fig. 1a), showing that the Global MERRA-2 winds agree well with the local radiosonde winds shown in Newman et al. (2016). The typical zonal wind pattern descent is interrupted by anomalous easterlies developing at 40 hPa in early 2016 along with the striking ascent of the westerly winds that began in late 2015. In comparison, the composite of the past 14 MERRA-2 QBO cycles (Fig. 1b) shows the typical descending shear zones. As in the longer radiosonde record (Newman et al. 2016) the global means show that the duration of the QBO westerlies at 40 hPa and easterlies at 10 hPa were approximately half of their typical duration.

The 2015-16 QBO anomaly with respect to the composite (Fig. 1c, the difference between Figs. 1a and b, with the annual and semi-annual cycles removed) shows the vertical extent and timing of the QBO disruption. The easterly anomaly at 40 hPa develops over the Nov 2015 – Apr 2016 time period along with the nearly simultaneous development of the westerly anomaly at 10 hPa. Note that the time scale for the appearance of the anomaly at all altitudes (a change over 15 km within a month) is much greater than the usual QBO descent time scale (1 km month^{-1}), another indication that the 2015-16 dynamics differ from the typical QBO dynamics. The standard deviation of the 14 QBO cycle composite (Fig. 1d) shows that most of the QBO variability usually occurs in the downward progressing shear zones in agreement with Pawson et al. (1993). Thus the downward westerly shear zone in 2014 and early 2015 shows expected variability, while the Dec 2015 and later anomaly pattern occurs in regions of weak vertical wind shear and generally low variability indicating an unexpected perturbation of the QBO.

Rossby wave activity propagation from the NH into the tropics is proportional to the negative of the horizontal momentum flux ($-\overline{u'v'}$, see Andrews et al. 1987, chapter 5). Figure 2 shows the time series of the 10°S–10°N, 40 hPa monthly averaged horizontal momentum flux (red curve) for the MERRA-2 time period. The largest peak is seen in the Dec 2015–Feb 2016 period. The Feb 2016 peak is about 50% greater than the Jan 2011 maximum. The Dec 2015 and Jan 2016 values are approximately the same as the Jan 2011 peak. Thus, the NH 2015-16 40 hPa level had the greatest Rossby wave activity observed in the 35-year MERRA-2 period.

The southward propagating Rossby waves led to the this historic deceleration of the tropical QBO westerelies. Fig. 2 shows the monthly averaged 10°S–10°N EP flux divergences or wind accelerations (blue curve), where negative values correspond to EP flux convergence and a negative, or easterly zonal wind acceleration. The large amplitude negative peak corresponds to Feb 2016, where there were large momentum fluxes (red curve) and an easterly acceleration of the equatorial winds (gray curve). As with the momentum fluxes, this peak is the largest seen at 40 hPa over the 35-year MERRA-2 period.

The mean flow changes can be traced backward to the subtropics using EP flux vectors. This wave propagation can be seen in the monthly mean winds and EP fluxes for the 2015–16 winter in Fig. 3. In November the equatorial QBO westerlies are centered at about 40 hPa with easterlies above. The November EP flux arrows show waves propagating into these westerlies, and across the equator — a pattern that is not atypical for QBO westerlies. However, as shown in Table 1 and discussed below, the momentum flux convergence is much stronger than in any of the previous westerly phases. December shows wave propagation across the equator and the start of small easterly perturbation intruding toward the equator. During the Jan–Feb period the westerlies are split into two maxima with development of easterlies at 40 hPa. In March the easterlies are fully developed, and continue to increase their vertical extent. By April, easterlies completely surround the separated upper westerly jet. During the Nov-Feb time period the average EP fluxes extended horizontally across the equator, indicating that Rossby waves, propagating from the sub-tropics and mid-latitudes, provided much of the forcing responsible for the zonal mean wind changes.

Nov-Dec 2015 still had equatorial westerlies at 40 hPa. Two years earlier, in Nov–Dec 2013, there were also equatorial westerlies at 40 hPa, however, the wave forcing was historically large during Nov–Dec 2015. This can be seen in Table 1 where the monthly mean momentum flux convergence between 10°S and 10°N is compared for these two NH winters. While the convergence is relatively small in November in both years, Dec 2015 is nearly seven times larger (5th row). The larger flux convergences continue into Jan–Mar with Jan 2016 nearly double and Feb 2016 nearly triple the 2014 values. Note that the Feb 2016 momentum flux convergence ($\sim$3 m s^{-1} month^{-1}) accounts for most of the 4.35 m s^{-1} month^{-1} February EP flux convergence (Fig. 2), indicating the importance of horizontal wave propagation in creating the disrupting easterlies.

Table 1 also compares the 2015–16 tropical moment flux convergence values to means and standard deviations of all the NH winter months with equatorial westerlies at 40 hPa. Months with equatorial westerlies have larger convergences than months with easterlies. Even so, the 2015–16 values are over three times larger than the mean values during Nov–Feb (6th row). The values seen in Dec–Mar 2015–16 are well over twice the standard deviation of past months (7th row). Only two NH winters during Jan 1980–Mar 2015 had months with momentum flux convergences greater than 2 m s^{-1} month^{-1} , Dec 1987, Feb 1988 and Dec 2010, Jan 2011, and these values were less than the Jan–Feb 2015 values.

Wave activity in the tropics was much higher during the 2015–16 QBO than during the comparable 2013-14 QBO. The increased wave activity in 2015 compared to 2013 is illustrated in Fig. 4, a plot of EPV at 40 hPa averaged over December. The same mean climate EPV field has been subtracted from both years to highlight the perturbations. From about 15°S to 30°N, southwest to northeast sloping, EPV anomalies are seen during 2015 (Fig. 4a) while 2013 shows smaller amplitude, more zonally oriented EPV anomalies. The zero zonal wind at this time is located at $\sim$15°S so the 2015 EPV orientations are consistent with positive momentum fluxes in the region of westerlies. Note that the SH vortex lasted late into Dec 2015 as denoted by the low EPV anomaly near the South Pole.

Fig. 4 shows only the time-averaged EPV features, however, transient waves also played a role in the stronger momentum flux values during the 2015–16 winter. Figure 5 shows an instantaneous (20 December 00 UTC) comparison of EPV fields for the two winters (2013–14, 2015–16) interpolated to the 530 K potential temperature surface. At this time, in the tropics, the 530 K potential temperature surface is at $\sim$40 hPa pressure altitude. The figure is colored to highlight (in green) the tropical EPV values. While tropical waves are present in both figures, the amplitudes (latitudinal extent) of the the disturbances are greater in 2015. There are approximately four waves present at this time (zonal wavenumber 4) though the spacing is irregular indicating a broad spectrum of zonal wavenumbers. These waves tilt from southwest to northeast with increasing longitude, indicating positive horizontal momentum fluxes and hence, north to south wave propagation. These tilts are much more apparent in 2015. Figure 5 is a frame taken from an animation covering the 2013–14 and 2015–16 Nov–Mar winters that is available as supplementary material.

While all the 2015–16 months had average or above average tropical momentum fluxes, the values for February 2016 were especially notable. Figure 6 shows the standard deviation normalized momentum and heat fluxes at 40 hPa as a function of latitude. The range of the previous Februaries (1980–2014) is given by the gray shading. The February 2016 momentum flux (Fig. 6a) is nearly 10 standard deviations above the climatology at 10°S. The next largest value is in 1983 at nearly 4 standard deviations, much less than the 2016 value. The 2016 momentum flux values are greater than 5 standard deviations from 20°S–15°N. As with the momentum fluxes the 2016 heat flux (Fig. 6b) stands out from the other years with only 1983 showing an equal peak value at 20°N (gray shading). Note that the 2016 heat fluxes are mainly positive north of the equator and negative south of the equator indicating upward wave propagation (vertical EP flux vectors) in both hemispheres.

Figure 7 shows February normalized momentum fluxes as a function of latitude and pressure for four selected years: 2016, 2014, 2011, and 1998. The large tropical values during 2016 are strongly focused at the 40 and 30 hPa levels with values greater than 9 standard deviations. February 2016 also shows relatively large positive values (>3) at 30°N and 100 hPa. The comparison year, 2014 (Fig. 7c), shows positive fluxes at 40 hPa in the tropics, however, they are much smaller (<2) than the 2016 values and most of the domain shows negative values. As in 2013–14, during 2010-11 westerlies continued throughout the winter, including February 2011 (Fig. 7c), however, February 2011 resembles 2014 more than 2016 with tropical momentum fluxes at 40 hPa peaking near 2 standard deviations. February 1998 (Fig. 7d), like 2014, was concurrent with a strong ENSO (El Niño Southern Oscillation) event along with westerlies in the equatorial lower stratosphere, however, the tropical values are more in agreement with 2014 and 2011 than with 2016. Overall, the 2014, 2011, and 1998 winters show negative momentum fluxes at 30°N and 100 hPa, in contrast to 2016.

Figure 8 compares the February heat fluxes for the same four years. The largest values (-5 to 4 standard deviations) are found in 2016 at 50 hPa in the tropics. As at 40 hPa (Fig. 6d), the field switches sign across the equator indicating a strong upward EP flux component over most of the tropics. There are also stronger positive and negative values during 2016 in the Northern Hemisphere upper troposphere (20-60°N, 150 hPa) than is seen in the other three years. Fig. 8 suggests that the tropical waves during 2016 are stronger than average, even in the Southern Hemisphere lower stratosphere. These results suggest that any waves propagating into the tropics or being forced in the tropics during 2016 would tend to propagate upward as well.

Along with strong tropical wave activity throughout the 2015–16 winter, there was an especially large amplitude tropical wave breaking event during early February 2016. Figure 9 shows the evolution of this feature in EPV on the 530 K potential temperature surface at 5 day intervals. The winter polar vortex (red shading) displayed a strong wavenumber 2 pattern on 31 January 2016 (Fig. 9a) that interacted with the tropical EPV (green shading) near 90°E longitude. This produced an intrusion of subtropical air (transparent shading) into the tropics and a wide-in-latitude "knot" of tropical EPV formed and propagated westward over equatorial Africa (Fig. 9b). By 10 February (Fig. 9c) the disturbance continued to propagate westward over the Atlantic Ocean and extended from South American to Africa. While the westward propagation slowed somewhat, 15 February found the EPV disturbance centered over South America with a long tail of tropical EPV extending south of the equator over the Western Pacific. (Note that an animation of Fig. 9 is available as supplemental material.)

As noted by Newman et al. (2016) and seen in Fig. 1 the normally downward propagating westerlies showed an upward propagation (or displacement) in 2016 at altitudes above $\sim$30 hPa in the lower stratosphere. Figure 10 plots the Dec 2015–Feb 2016 vertical component of the residual mean circulation (with multi-year means removed), $\overline{w}^*$. The calculated $\overline{w}^*$ field shows upward motion above $\sim$40 hPa centered at $\sim$5°S. The upward values of $\sim$1 km month^{-1} are the same order of magnitude as the observed upward displacement and suggest that the meridional circulation response to the easterly acceleration at 40 hPa played a major role in the observed upward displacement.

4. Summary and Conclusions

The disruption of the QBO mean zonal wind during the 2015–16 NH winter was associated with record strong stratospheric tropical wave activity. This disruption was well captured by MERRA-2 (Fig. 1). The mean wind disruption was the most dramatic seen since regular observation of the QBO began (Newman et al. 2016). Associated with this record disruption, the tropical wave momentum flux at 40 hPa, after very strong values during Dec–Jan, attained a record peak value in Feb 2016 (Fig. 2), the largest in magnitude of any month during the 35-year MERRA-2 time period. This tropical wave activity was especially focused at the 40 hPa level (Figs. 6 and 7). Initially in Nov–Dec 2015, the wave momentum fluxes crossed the equator, reaching the SH easterlies. The SH easterlies at 40 hPa then intruded toward and eventually crossed the equator, effectively splitting the QBO westerlies (Fig. 3).

In summary, the boreal winter of 2015-16 showed:

- record strong momentum and heat fluxes in the tropical lower stratosphere consistent with southerly and upward wave propagation.
- the lower stratosphere QBO westerlies were split vertically from south to north in time.
- a large amplitude tropical wave breaking event occurred in February 2016.

There is still the question of what forced the NH wave generation necessary to cause the 2015–16 QBO disruption. Comparisons with the next most recent QBO westerly NH winter (2013–14) also showed waves in the equatorial region (Table 1 and Figs. 4 and 5). However, in 2013–14 the waves were not of sufficient magnitude to disrupt the QBO, and westerlies prevailed throughout the winter. The 2015–16 increased wave forcing could have resulted from the naturally large stratospheric-tropospheric internal variability, or possibly be tied to specific variability such at that associated with ENSO or changed global climate patterns. In particular Newman et al. (2016)

(their Fig. 4) showed that the tropical upper tropospheric temperatures were much warmer than the MERRA-2 climate record. Such warm temperatures may affect tropical and middle latitude wave generation and propagation.

Along with the specific cause of the increased wave forcing there is the need to understand why the waves were focused near 40 hPa in altitude. This wave focusing allowed the full wave-induced easterly acceleration to be applied consistently over several months, adding up to the significant rearrangement of the tropical lower stratospheric winds by the end of March 2016. One possibility is to examine the so-called refractive index (Matsuno 1970) to identify subtle differences in wave propagation pathways between 2015-16 and previous winters. The intrusion of the easterlies resulting from Rossby waves is unexpected given the modeling results of O'Sullivan (1997) generally showing only changes in the zonal mean wind gradients and not the equatorial jet maximum. However, O'Sullivan (1997) also showed that, for one choice of modeling parameters, the QBO westerly jet maximum was reduced. Future work could consider a wider range of model parameters to better characterize the conditions under which Rossby waves can significantly alter the QBO jet.

More detailed diagnostic and model forecast studies are needed to resolve meridional circulation changes associated with this 2015-16 disrupted QBO and to test the ability of seasonal forecast systems to encompass and predict such a disruption of the QBO. The splitting of the easterlies and the upward progression of the westerlies will also disrupt the QBO mean meridional circulation Plumb and Bell (1982) and hence the transport and distribution of stratospheric trace gases and aerosols. In particular, the upward progression of westerlies observed may be a direct response to induced changes in the mean meridional circulation (Fig. 10). Along with developing the ability to forecast a major disruption of the QBO, this event may require re-evaluation of the QBO seasonal prediction skill (Scaife et al. 2014).

Acknowledgments. This research was performed with funding from the NASA Modeling, Analysis and Prediction program and the NASA Atmospheric Composition Modeling and Analysis Program. The MERRA-2 reanalysis fields were obtained from the NASA Earth Observing System Data and Information System (https://earthdata.nasa.gov). The specific MERRA-2 fields used are listed in the references.

References

Andrews, D. G., J. R. Holton, and C. B. Leovy, 1987: *Middle Atmosphere Dynamics*. Academic Press, 489 pp.

Baldwin, M. P., and Coauthors, 2001: The quasi-biennial oscillation. *Rev. Geophys.*, **39**, 179–229.

Bosilovich, M. G., and Coauthors, 2015: MERRA-2: Initial Evaluation of the Climate. NASA Tech. Rep. Series on Global Modeling and Data Assimilation, NASA/TM-2015-104606, Vol. 39, NASA, 136 pp.

Coy, L., K. Wargan, A. M. Molod, W. R. McCarty, and S. Pawson, 2016: Structure and dynamics of the quasi-biennial oscillation in MERRA-2. *J. Clim.*, **29**, 5339–5354, doi:10.1175/JCLI-D-15-0809.1.

GMAO, 2015a: Global Modeling and Assimilation Office, inst3 3d asm Nv: MERRA-2 3D Assimilated Meteorological Fields 3-hourly (model level, 0.625x0.5L42), version 5.12.4. Greenbelt, MD, USA: Goddard Space Flight Center Distributed Active Archive Center (GSFC DAAC), accessed June 2016, doi:10.5067/WWQSXQ8IVFW8.

GMAO, 2015b: Global Modeling and Assimilation Office, instM 3d asm Np: MERRA-2 3D IAU State, Meteorology Monthly Averaged 3-hourly (p-coord, 0.625x0.5L42), version 5.12.4.

Greenbelt, MD, USA: Goddard Space Flight Center Distributed Active Archive Center (GSFC DAAC), accessed June 2016, doi:10.5067/2E096JV59PK7.

Hamilton, K., 1982: Some features of the climatology of the Northern Hemisphere stratosphere revealed by NMC upper atmosphere analyses. *J. Atmos. Sci.*, **39**, 2737–2749, doi:http://dx.doi.org/10.1175/1520-0469(1982)039⟨2737:SFOTCO⟩2.0.CO;2.

Holt, L. A., M. J. Alexander, L. Coy, A. Molod, W. Putman, and S. Pawson, 2016: Tropical waves and the quasi-biennial oscillation in a 7-km global climate simulation. *J. Atmos. Sci*, in press.

Kawatani, Y., K. Hamilton, K. Miyazaki, M. Fujiwara, and J. A. Anstey, 2016: Representation of the tropical stratospheric zonal wind in global atmospheric reanalyses. *Atmos. Chem. Phys.*, **16**, 6681–6699, doi:10.5194/acp-16-6681-2016.

Lindzen, R. S., and J. R. Holton, 1968: A theory of the quasi-biennial oscillation. *J. Atmos. Sci.*, **25**, 1095–1107.

Matsuno, T., 1970: Vertical propagation of stationary planetary waves in the winter Northern Hemisphere. *J. Atmos. Sci.*, **27**, 871–883, doi:http://dx.doi.org/10.1175/1520-0469(1970)027⟨0871:VPOSPW⟩2.0.CO;2.

Molod, A., L. Takacs, M. Suarez, and J. Bacmeister, 2015: Development of the GEOS-5 atmospheric general circulation model: Evolution from MERRA to MERRA2. *Geosci. Model Dev.*, **8**, 1339–1356, doi:doi:10.5194/gmd-8-1339-2015.

Newman, P. A., L. Coy, and S. Pawson, 2016: The unusual quasi-biennial oscillation structure of 2016. *Geophys. Res. Lett.*, submitted.

O'Sullivan, D., 1997: Interaction of extratropical Rossby waves with westerly quasi-biennial oscillation winds. *J. Geophys. Res.*, **102**, 19 461–19 469.

Pawson, S., K. Labitzke, R. Lenschow, B. Naujokat, B. Rajewski, M. Wiesner, and R.-C. Wohlfart, 1993: Climatology of the Northern Hemisphere stratosphere derived from Berlin analyses. Part 1: Monthly means. Neue folge, ser. a, Meteorologische Abhandlungen der Freien Universität Berlin.

Plumb, R. A., and R. C. Bell, 1982: A model of the quasi-biennial oscillation on an equatorial beta-plane. *Q.J.R. Meteorol. Soc.*, **108**, 335–352, doi:10.1002/qj.49710845604.

Scaife, A. A., and Coauthors, 2014: Predictability of the quasi-biennial oscillation and its northern winter teleconnection on seasonal to decadal timescales. *Geophysical Research Letters*, **41 (5)**, 1752–1758, doi:10.1002/2013GL059160, URL http://dx.doi.org/10.1002/2013GL059160, 2013GL059160.

LIST OF TABLES

TABLE 1. Comparison of MERRA-2 monthly equatorial (10°S-10°N) momentum flux convergence at 40 hPa for 2015–16 and 2013–14 in m s^{-1} $month^{-1}$. Third and forth row are the mean and standard deviations of the flux convergence for all the months (Jan 1980–Mar 2015) with westerly zonal mean zonal winds at 40 hPa (m s^{-1} $month^{-1}$). Negative values denote easterly acceleration. Bottom three rows give the non-dimensional ratio of 2015–16 (top row) values to the values in rows 2–4 respectively.

	Nov	*Dec*	*Jan*	*Feb*	*Mar*
2015-16	-0.75	-1.98	-2.69	-2.99	-1.48
2013-14	0.07	-0.29	-1.38	-1.08	-0.87
Mean (W)	-0.13	-0.56	-0.83	-0.85	-0.52
StdDev (W)	0.43	0.80	0.73	0.64	0.54
Ratio (15/13)	11.33	6.88	1.95	2.78	1.70
Ratio (15/W)	5.70	3.55	3.23	3.51	2.86
Ratio (15/SD)	1.75	2.48	3.69	4.67	2.76

LIST OF FIGURES

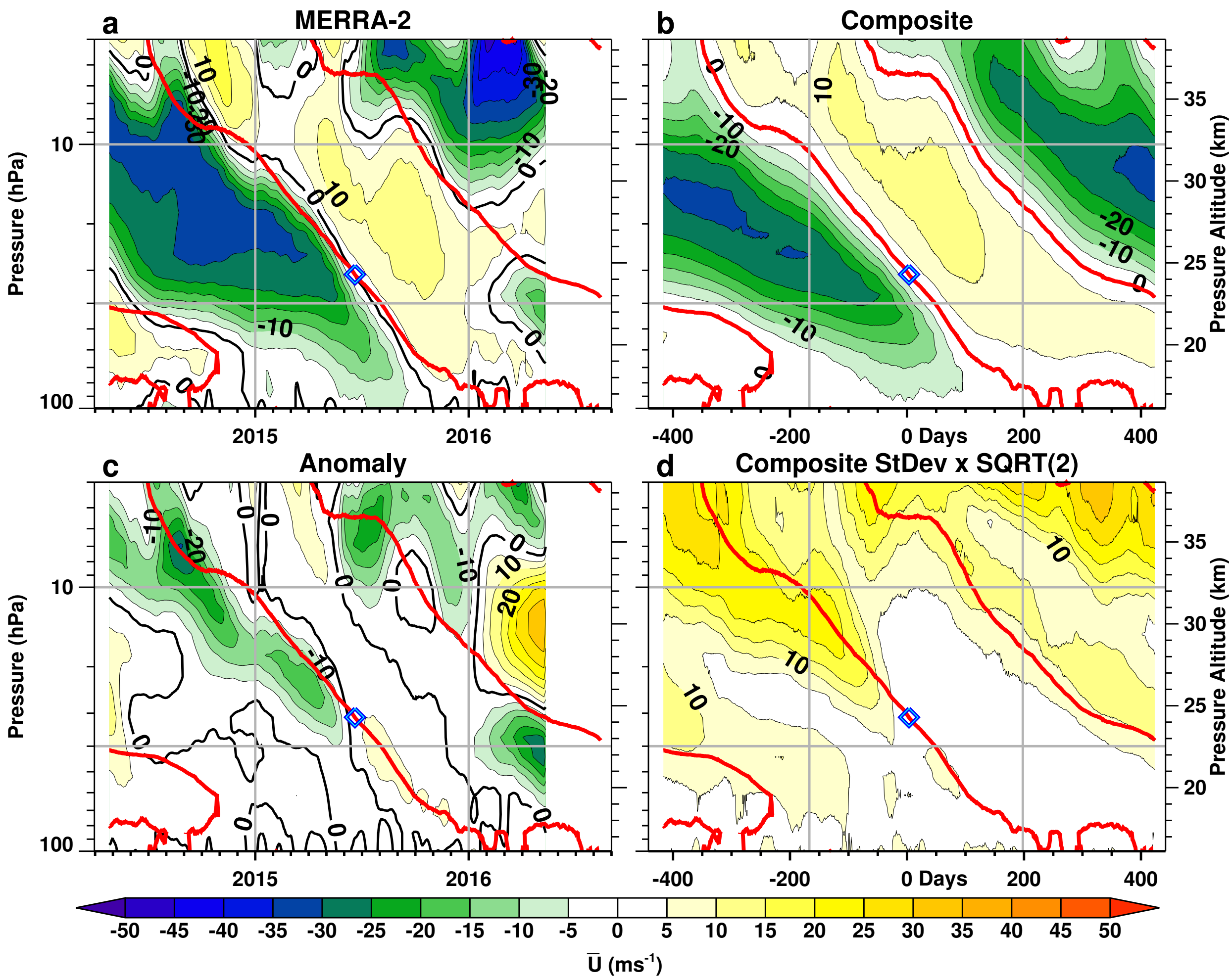

FIG. 1. Zonal mean zonal wind component, $\overline{u}$ (m s^{-1}), as a function of time and pressure: a) MERRA-2 wind analysis from May 2014 to May 2016, b) MERRA-2 composite based on 14 easterly to westerly wind transitions at 30 hPa, c) the wind analysis fir 2915–2016 minus the composite, and d) the standard deviation ($\times\sqrt{2}$) of the 14 composite members. The red contours denote the composited zero wind. The Blue diamond denotes the compositing reference point. The winds are averaged from 10°S–10°N.

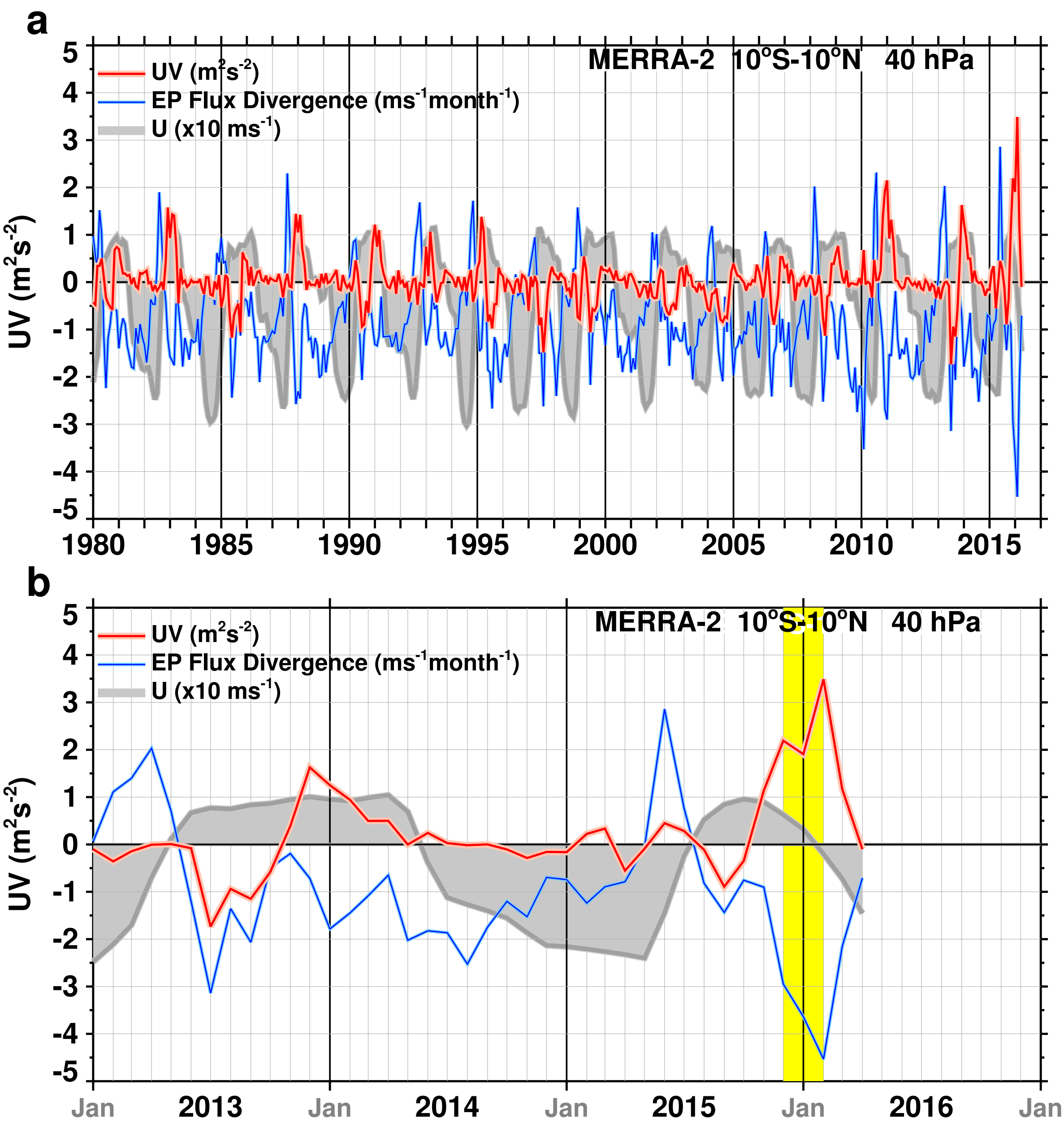

FIG. 2. a) January 1980 to May 2016, monthly averaged, 10°S–10°N averaged, 40 hPa, MERRA-2, momentum flux (red, m^2s^{-2}), EP flux divergence (blue, m s^{-1}month^{-1}), and zonal mean zonal wind (gray, $\times$10 m s^{-1}). Vertical lines denote the start of a year; b) expanded time coordinate to highlight years 2013–2016. Yellow shading denotes months Dec 2015–Feb 2016.

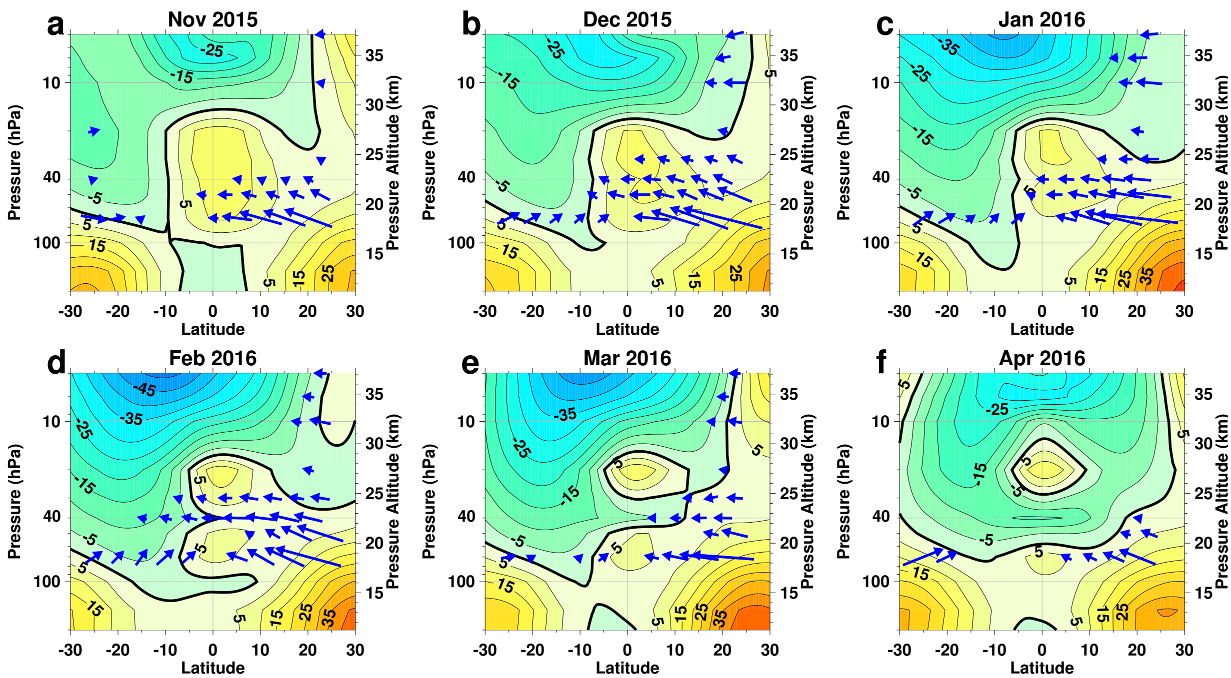

411 FIG. 3. Monthly averaged zonal mean zonal wind plotted from 30°S-30°N and from 200–4 hPa for the months:
412 a) Nov 2015, b) Dec 2015, c) Jan 2016, d) Feb 2016, e) Mar 2016, and f) Apr 2016. Westerlies are yellow-red
413 and easterlies are green-blue with 5 m s^{-1} contours. Also plotted are the EP flux vectors (blue arrows) at 70 hPa
414 and above.

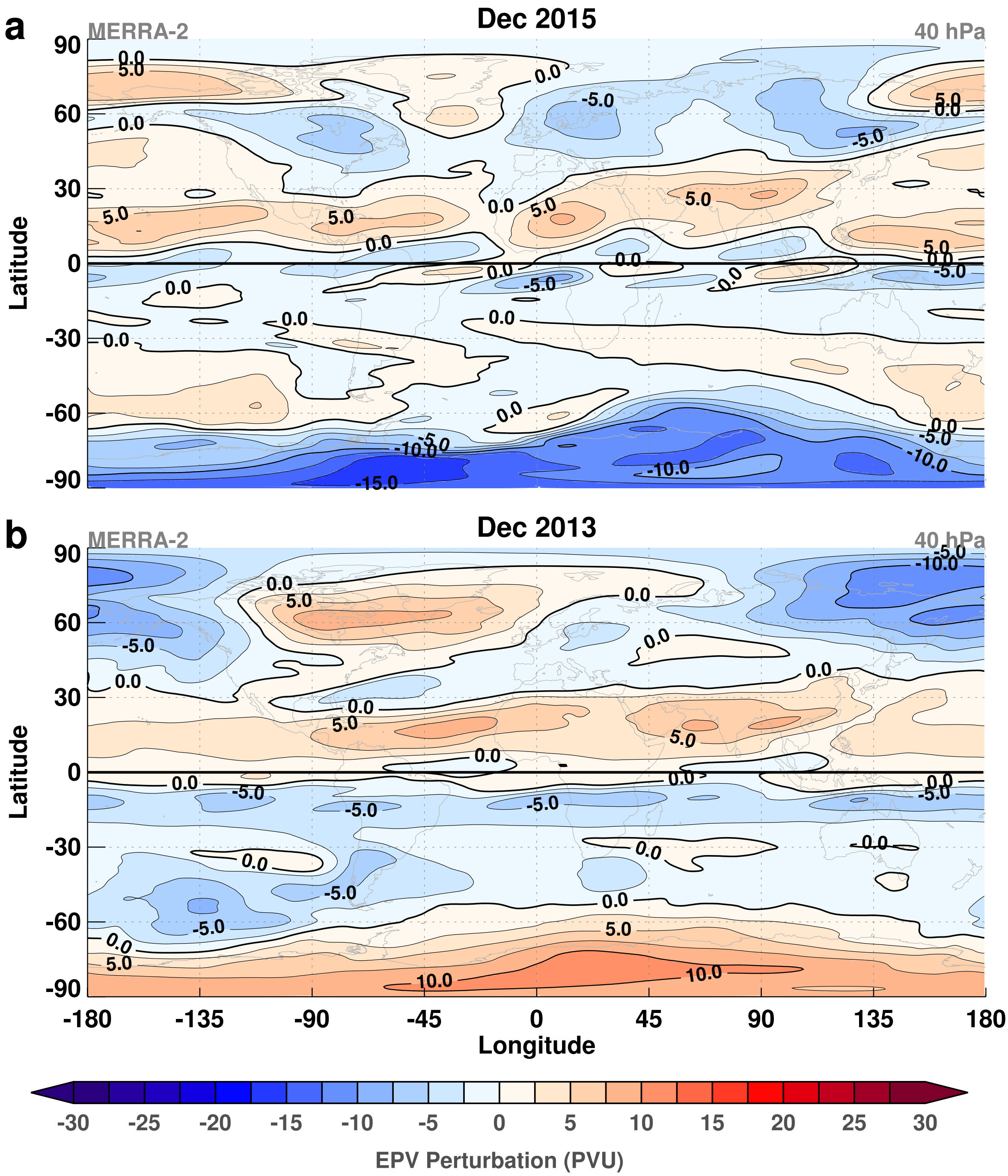

415 FIG. 4. The December monthly average EPV (1 Potential Vorticity Unit, PVU = 10^{-6} m^2 s^{-1} K kg^{-1}) at 40 hPa with the December MERRA-2 climate mean (1980–2014) subtracted for a) 2015 and b) 2013.

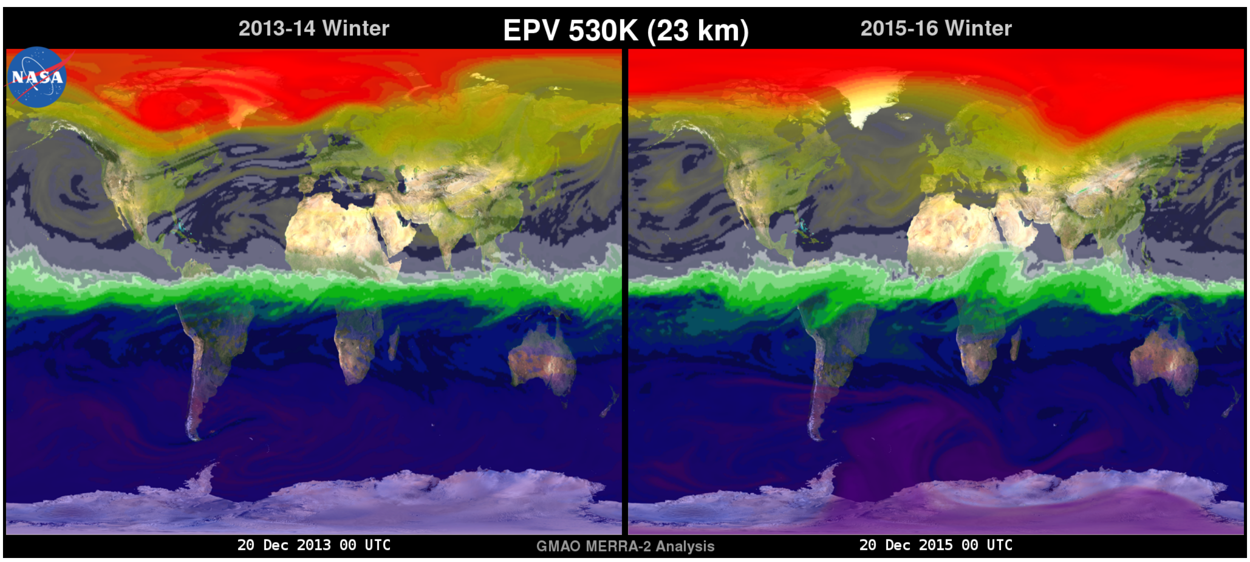

FIG. 5. EPV (1 Potential Vorticity Unit, PVU = 10^{-6} m^2 s^{-1} K kg^{-1}) on the 530 K potential temperature surface for 20 December 00 UTC 2013 (left) and 2015 (right). The green colors denote values from $\sim$ -15–15 PVU, red denote values >100 PVU, and purple denote values <-50 PVU. The 530 K surface is approximately at 40 hPa near the equator.

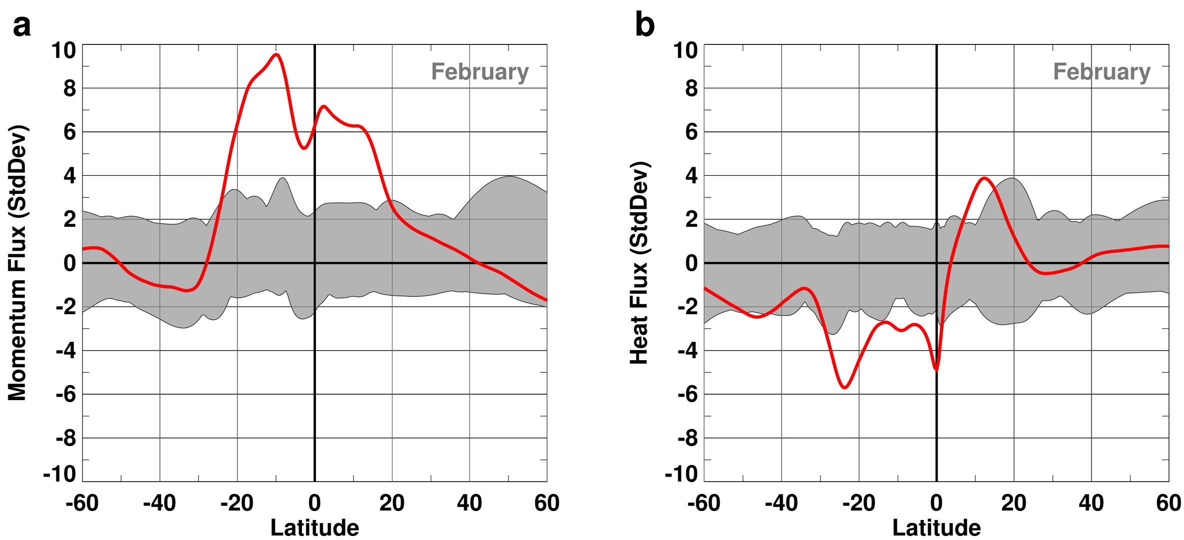

421 FIG. 6. Zonally averaged momentum (a) and heat (b) fluxes at 40 hPa for February 2016 (red curve, 10°S-10°N) and plotted as functions of latitude. The values are non-dimensional in terms of standard deviations over the years 1980–2014. The gray shaded regions denotes the February normalized range over 1980–2014.

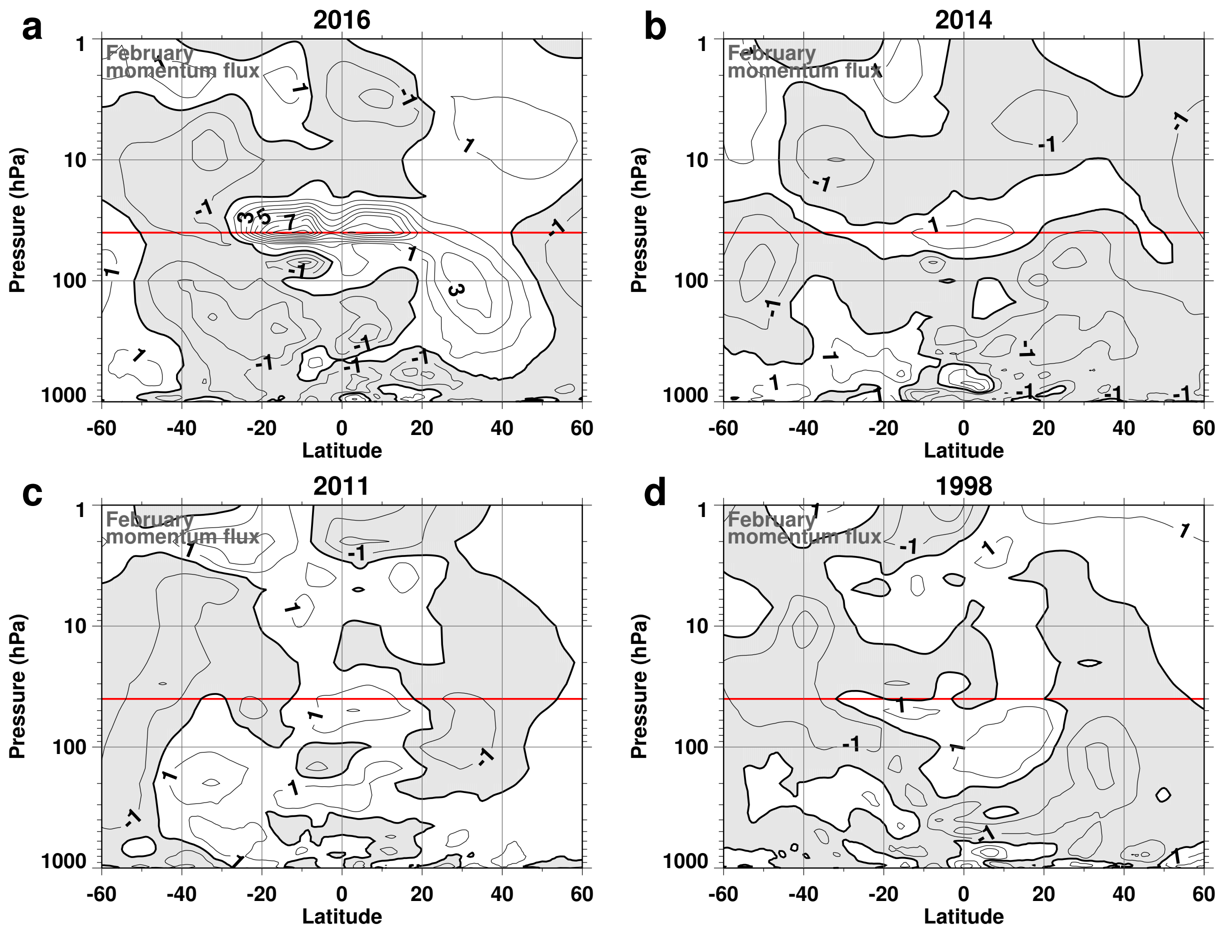

424 FIG. 7. February zonally averaged momentum flux for a) 2016, b) 2014, c) 2011, and d) 1998 as function of
425 latitude and pressure. The values are non-dimensional in terms of standard deviations over the years 1980–2014
426 with a contour interval of one standard deviation. Negative values are shaded gray. The red horizontal line
427 denotes the 40 hPa level.

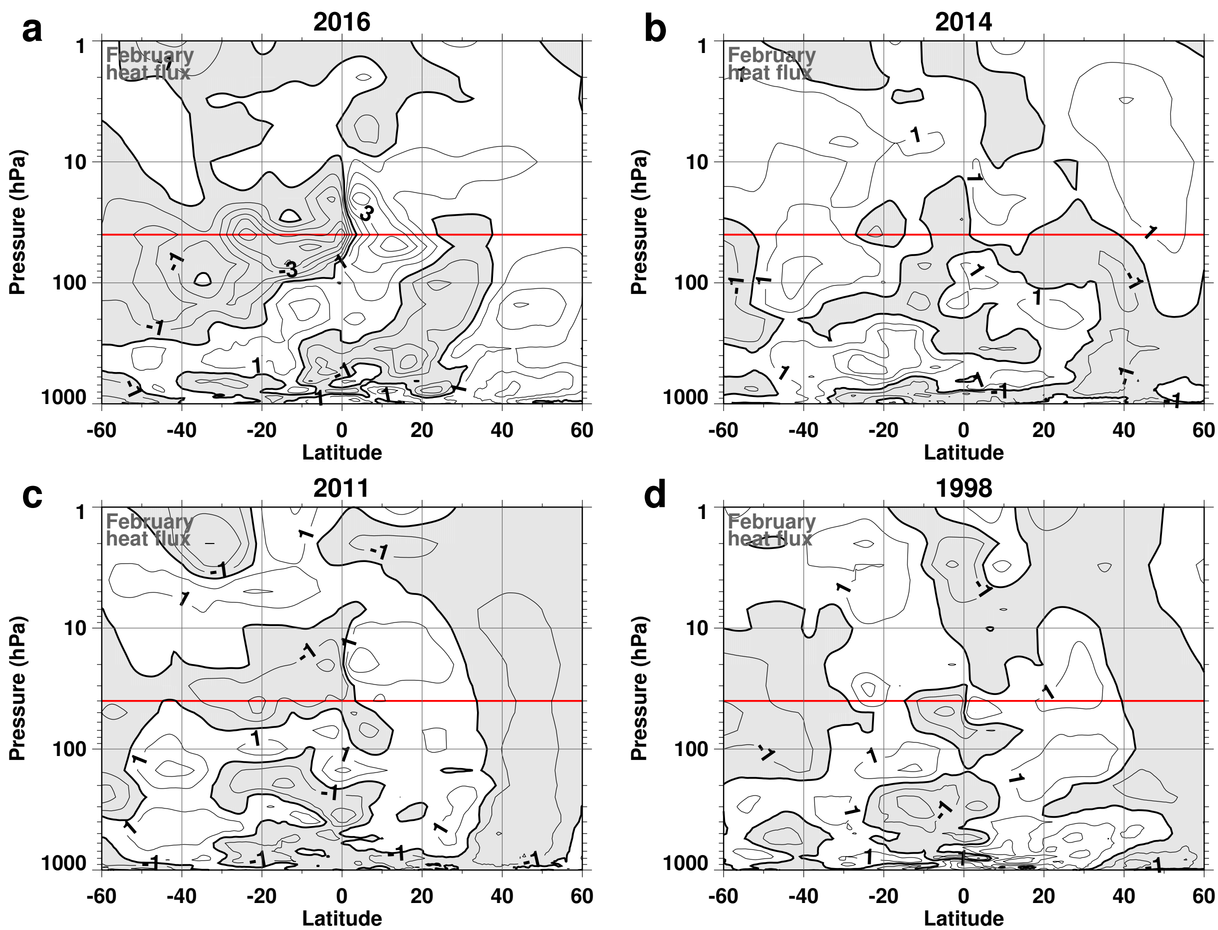

FIG. 8. Same as Fig. 7 for heat flux.

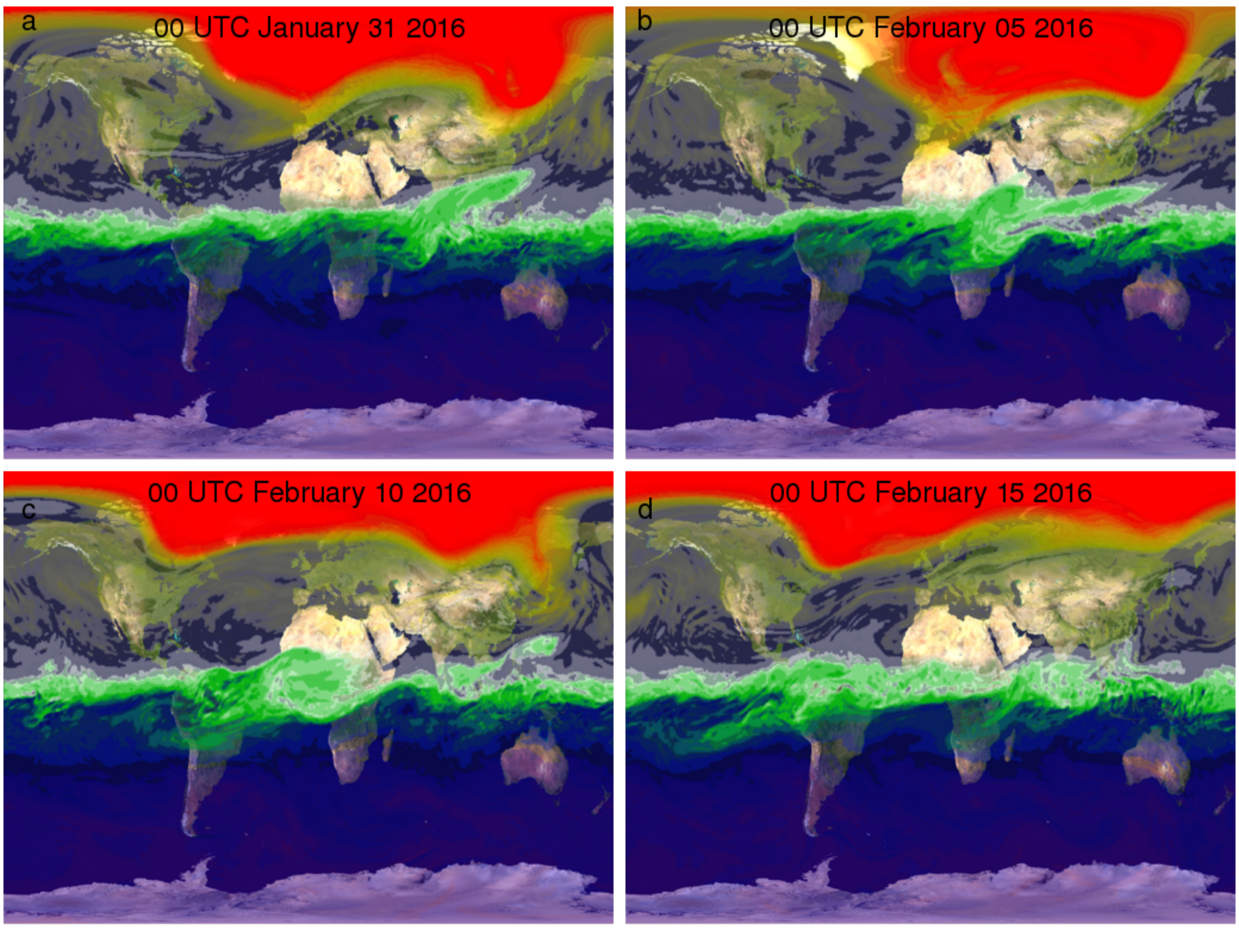

FIG. 9. EPV on the 530 K potential temperature surface for 00 UTC on a) January 31, b) February 5, c) February 10, and d) February 15 of 2016. Colors are as in Fig. 5.

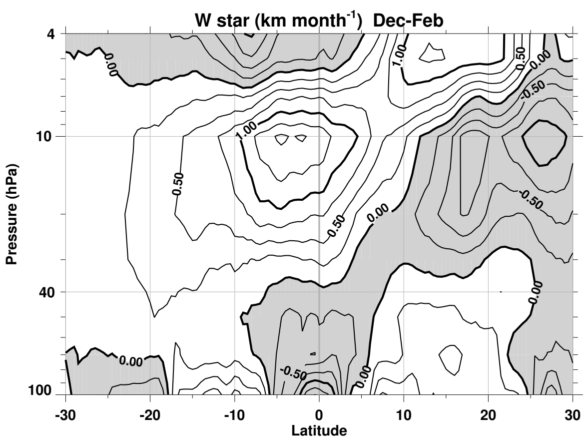

FIG. 10. The vertical component of the residual mean circulation (km month^{-1}) averaged Dec 2015 – Feb 2016 as a function of latitude and pressure. The multi year (Dec 1980– Feb 2015) monthly means have been subtracted. Negative values are shaded.

Click here to access/download

Supplemental Material

epv_530_1314_1516_m2.mp4